Organic Electronics 13 (2012) 215–221

Contents lists available at SciVerse ScienceDirect

Organic Electronics

journal homepage: www.elsevier.com/locate/orgel

BODIPY derivatives as n-type organic semiconductors: Isomer effect on carrier mobility

Ming-Xing Zhang, Shuo Chai, Guang-Jiu Zhao *

State Key Laboratory of Molecular Reaction Dynamics, Dalian Institute of Chemical Physics, Chinese Academy of Sciences, 457 Zhongshan Road, Dalian 116023, China

ARTICLE INFO

Article history:
Received 2 September 2011
Received in revised form 21 October 2011
Accepted 23 October 2011
Available online 19 November 2011

Keywords:
Carrier mobility
Organic semiconductor
BODIPY
Electron transfer
Isomer effect
Anisotropic behavior

ABSTRACT

In the present work, two dipyrro-boradiazaindacenes (BODIPY) derivatives functioning as novel high-performance organic semiconductors are investigated by theoretical method. These two isomeric complexes are demonstrated to have large electron-transfer mobility, which means they are favor to be n-type organic semiconductors. The highest electron-transfer mobility appears at the same packing style in two crystals. The intermolecular distances of the packing style are nearly same, 4.994 Å in crystal 1 and 5.283 Å in crystal 2. However, their electron-transfer mobility changes significantly. The mobility of crystal 2 with better planar molecular structure is 0.291 $cm^2\,V^{-1}\,s^{-1}$, which is 13 times larger than that of crystal 1 as 0.022 $cm^2\,V^{-1}\,s^{-1}$. The significant difference of carrier mobility is ascribed to the little structural difference of these two isomers. It has been demonstrated that both crystal 1 and 2 show remarkable anisotropic behavior. This study will undoubtedly provide a new understanding of isomerization on designing novel organic semiconductors.

1. Introduction

In the past decades, molecular organic semiconductors is the object of much interest because of their applications in new generations of (opto)electronic devices [1–8]. The development of single-crystal organic field effect transistors (SCOFETs) makes it possible to explore intrinsic properties of these materials [9–11]. p-Type organic semiconductors such as pentacene, rubrene and derivatives of them have been investigated widely [12–27]. The recently improved theoretical understandings of organic semiconductors have even addressed the design rule of organics with high hole mobilities [28–31]. However, n-type semiconductors are not fully developed, and their field effect transistors (FETs) performance is not satisfactory yet. Fluorinated perylene diimide as a novel organic n-type material was reported by Heremans and coworkers in 2005 [32]. They also did research on the influence of the contact metal on the performance of n-type carbonyl-functionalized quaterthiophene organic thin-film transistors [33]. Kahn and coworkers used direct and inverse photoemission spectroscopy and some other experimental methods to study the n-type doping of an electron transport materials in 2006 [34,35]. Recently, they have reported a new acetylenic n-type organic semiconductor: fluoro-substituted phenyleneethynylenes with high performance [36]. Among intrinsic properties of organic semiconductors, the electrical anisotropy of organic materials has attracted much attention [9,37–47]. The anisotropic effects in rubrene crystals were first observed by Sundar et al. in 2004 [9]. Deng and Han have investigated the quantitative structure–activity relationships of transport properties in a series of organic semiconductors such as acene, acene derivatives and rubrene by first-principles-based simulation based on Marcus-Hush theory [48–51]. They provide systematically anisotropic mobility of each

---

* Corresponding author. Tel.: +86 411 84379692; fax: +86 411 84675584.
E-mail address: gjzhao@dicp.ac.cn (G.-J. Zhao).

1566-1199/$ - see front matter © 2011 Elsevier B.V. All rights reserved.
doi:10.1016/j.orgel.2011.10.015

material above, which agree with experiments very well [48–51].

As we all know, dipyrro-boradiazaindacenes (BODIPY) is fluorescence sensor with good function. The properties of BODIPY and its derivatives have been studied widely [52–58]. Herein, we investigate the properties of two derivatives of BODIPY function as organic semiconductor. These two compounds are isomers with only little difference of the structure as shown in Fig. 1. Our simulations demonstrate that this kind of BODIPY derivative has better mobility function as n-type organic semiconductor comparing with p-type. On the other hand, complex 2 has larger electron mobility than complex 1, though there's only little different of their monomers and crystal structures. This obvious difference indicates that isomerization has significant influence on the mobility. The favorable performance as n-type organic semiconductor of both complex 1 and 2 is assigned to the high electron affinity of F atoms in the molecule. The better planar structure of complex 2 is demonstrated to be responsible for large electron mobility of crystal 2.

2. Theory and computational methods

Our simulation model is based on first-principle quantum mechanics (QM) calculations combined with Marcus-Hush theory [59,60]. For the calculations of the intermolecular effective electronic coupling, we calculate the spatial overlap (S_{ij}), charge transfer integrals (J_{ij}), and site energies (e_i, e_j):

$$e_{(}ij) = \langle \psi_{i(j)} \mid H \mid \psi_{(i)j} \rangle \tag{1}$$

$$S_{(ij)} = \langle \psi_i \mid \psi_j \rangle \tag{2}$$

$$J_{ij} = \langle \psi_i \mid H \mid \psi_j \rangle \tag{3}$$

where H is the system Kohn–Sham Hamiltonian of the dimer system, and $\Psi_{i(j)}$ means the monomer HOMOs (for hole transport) or LUMOs (for electron transport) with Löwdin's symmetric transformation, which can be used as the orthogonal basis set for calculation [61]. Then the intermolecular electronic coupling V_{ij} can be written as

$$V_{ij} = (J_{ij} - 0.5(e_i + e_j)S_{ij})/(1 - S_{ij}^2) \tag{4}$$

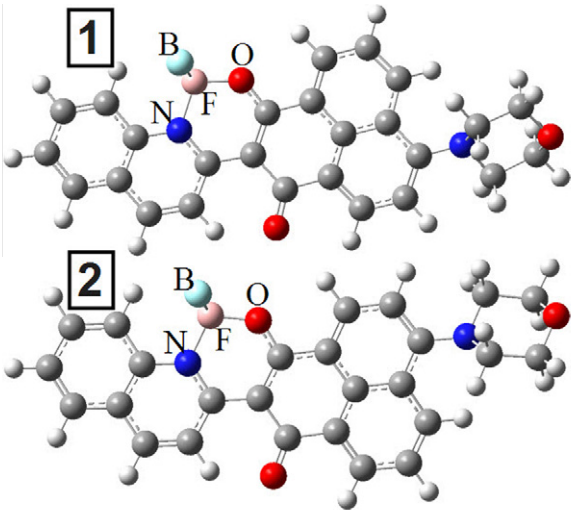

Fig. 1. Optimized structures of monomer 1 and 2 in crystal 1 and 2, respectively.

The calculations of all electronic couplings in different molecular packing dimers are performed with the PW91/TZ2P of density functional theory (DFT) implemented in the Amsterdam density functional (ADF) program [62]. The reorganization energy λ associated with charge transport process in organic solid materials is evaluated by the adiabatic potential energy surface method:

$$\lambda = (E_+^* - E_+) + (E^* - E) \tag{5}$$

or

$$\lambda = (E_-^* - E_-) + (E^* - E) \tag{6}$$

where E and E_+ (E_-) represent the energies of the neutral and cation (anion) species in their lowest energy geometries, respectively; E^* are the energies of the neutral and cation (anion) species with the geometries of the cation (in Eq. (5)) and anion (in Eq. (6)). E_+^* (E_-^*) are the energies of cation (anion) species with the geometries of neutral species, respectively. Then the adiabatic ionization potential (IP) and affinities (EA) can be calculated as

$$IP = E_+ - E \tag{7}$$

$$EA = E_- - E \tag{8}$$

Full geometry optimizations of the monomer molecules and the reorganization energy calculations are carried out using the B3LYP functional in conjunction with the 6-31G(d,p) basis set [63]. These calculations are performed with the Gaussian09 package [64]. The reorganization energy consists of intra- and intermolecular contributions. Here we focus on the intramolecular contributions. However, the neglect of intermolecular contribution of reorganization energy will result in the overestimation of the hopping rate Eq. (10) and sequentially the absolute value of mobility Eq. (9) and (11). Previous research [65] suggested a method to evaluate the intermolecular geometric relaxation energy based on the electronic polarization P_+ that results from the interaction of the excess charge with both permanent and induced multipoles in surrounding molecules, and the P_+ can be obtained from the ultraviolet photoelectron spectroscopic (UPS) data of gas and solid phases [66,67]. Herein, we pay our attention to indicate which kind of organic semiconductor complex 1 and 2 could be function as, the n-type or p-type and which one has better functions. The total same method is chose for calculation of each compound. Therefore, the systematic error will be eliminated by comparison and the absolute value is not so important. At room temperature, it is generally accepted that the transport in organic materials occures via charge carrier hopping between adjacent molecules. Assuming no correlation between charge hopping events and charge motion is a homogeneous random walk, the maximum values of drift mobility for charge carrier (hole/electron) transport in semiconductor can be written as [28,49].

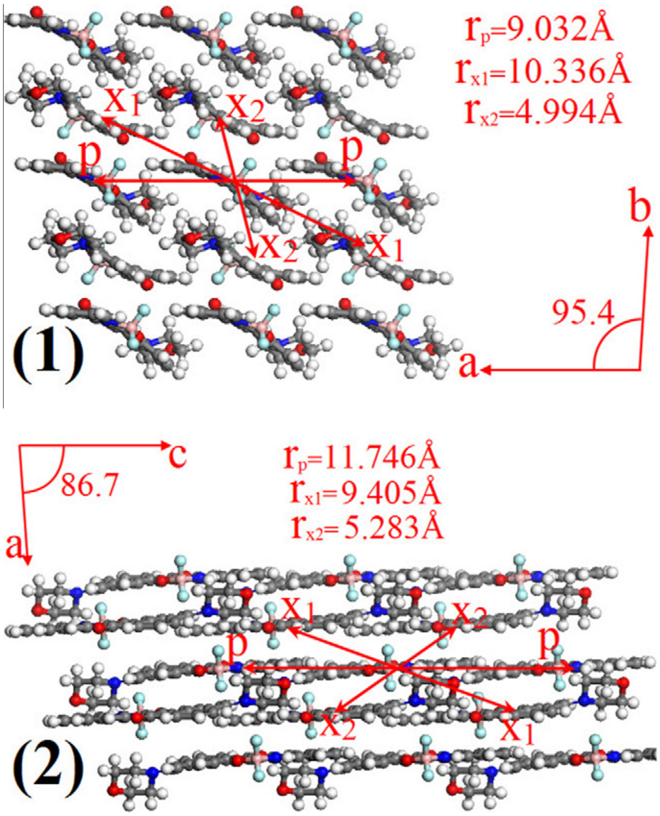

Fig. 2. Illustration of charge hopping pathway schemes in the same molecular stacking layers in (1) for crystal 1 and (2) for crystal 2.

$$\mu = \frac{e}{k_BT}D = \frac{e}{k_BT}\lim_{t\to\infty}\frac{1}{2n}\frac{\langle x(t)^2\rangle}{t} \approx \frac{e}{2nk_BT}\sum_i r_i^2 W_i P_i \tag{9}$$

where n is the spatial dimensionality, r_i is the hopping distance; P_i is the hopping probability, $P_i = W_i/\sum_i W_{ij}$, i means the ith pathway; W is the intermolecular hopping rate based on Marcus-Hush theory [68] in the high-temperature limit:

$$W = \frac{V^2}{\hbar}\left(\frac{\pi}{\lambda k_BT}\right)^{1/2} \exp\left(-\frac{\lambda}{4k_BT}\right) \tag{10}$$

λ is the reorganization energy and V is the intermolecular effective electronic coupling. The magnitude of the field effect mobility in a particular transistor channel depends on the specific surface of the organic crystal. We analyze the mobility of components for each surface in terms of angles of the hopping jumps (γ_i) between adjacent molecules relative to the plane of interest. Crystal 1 and 2 give rise to a two-dimensional (2D) transport within the basal stacked organic layers, while transport between layers is less efficient; the values of γ_i are 0°. Using the basal plane as the reference, Φ is the orientation angle of the transistor channel relative to the reference axis (generally using the crystallographic axis) and $\{\theta_i\}$ are the angles of the projected electronic coupling pathways of different dimer types relative to the reference axis. Thus, the angles between the different pathways and the conducting channel are $\theta_i - \Phi$, as shown in Fig. 4a for crystal 1 and Fig. 4b for crystal 2. We then use projection to describe the combined effects of different electronic coupling pathways on every measuring transistor channel Φ. In the basal stacked organic layers of crystal 1 and 2, neighboring molecules can be characterized as transverse dimers X_1, X_2 and parallel dimers P, as illustrated in Fig. 2. For the ideal high-purity crystals without disorder, the orientations of the molecules surrounding each molecule are identical, so that Eq. (9) leads to the orientation function describing the mobility in a specific conducting direction on a specific surface in organic single crystal [28,49].

$$\mu_\phi = \frac{e}{2k_BT}\sum_i W_r r_i^2 P_i cos^2\gamma_i cos^2(\theta_i - \Phi) \tag{11}$$

where r_i is the hopping distance; $P_i cos^2\gamma_i cos^2(\theta_i - \Phi)$ describes the relative hopping probability of various electronic coupling pathways to the specific transistor channel; γ_i and θ_i are determined by the molecular architecture in the organic crystal. In Eq. (11), a specific Φ corresponds to a specific conducting direction; thus, the spatial dimensionality n in Eq. (9) is taken to be approximately 1 to extract the mobility along a specific direction for the derivation of Eq. (11). Eq. (11) can be considered as an anisotropic three-dimensional random walk with the charge drifting effect in one direction, and it provides an analytic function to determine the angular resolution

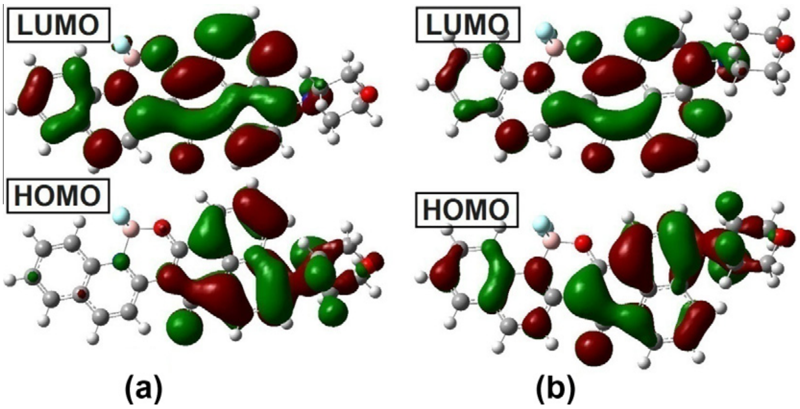

Fig. 3. Frontier molecular orbitals of complex 1 (a) and 2 (b).

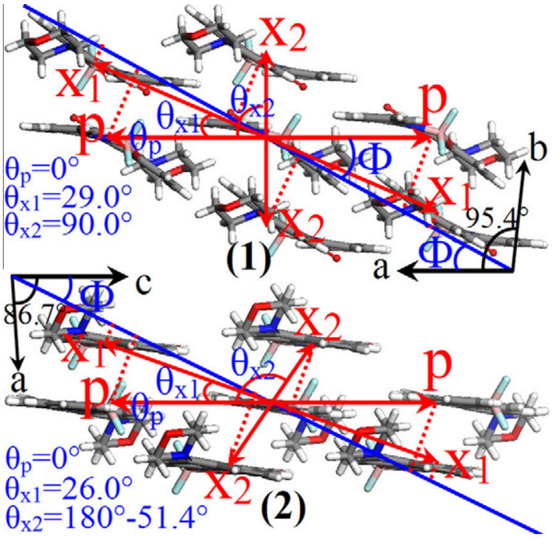

Fig. 4. Illustration of dimmers models in crystal 1 and 2, (1) for crystal 1 and (2) for crystal 2.

anisotropic mobilities for any type of organic semiconductors by relating the crystal packing and electron coupling V to the outer measuring channel angle Φ.

3. Results and discussion

As shown in Fig. 1, monomers of crystal 1 and 2 have the same formula $C_{26}H_{19}BF_2N_2O_3$, but molecular structures are somewhat different. The heterocycle associates with C1 in monomer 1, while it is C2 in monomer 2. The main part of the molecule 2 is more planar than molecule 1 which means the π-conjugation of molecule 2 should be larger than molecule 1. The calculated energies of these two monomers are similar. The reorganization energies λ_- of complexes 1 and 2 are 0.290 and 0.316 eV, respectively, while λ_+ are 0.529 and 0.475 eV. It's easy to find that λ_- of 1 and 2 are both smaller than λ_+. High reorganization energy is unfavorable for higher carrier mobilities [26,69,70]. Thus, complex 1 and 2 are proposed to function as a more high efficiency n-type organic semiconductor than p-type.

Another important parameter of charge transfer ability of a material is the intermolecular electronic coupling V. For crystal 1 and 2, four types of intermolecular packing modes are defined as X1, X2, P, and L. The X1,X2, and P dimers are in the same molecular stacking layer as shown in Fig. 2, and head-to-tail stacking (L dimers) is out of the molecular stacking layer of X1, X2, and P dimers. As used in Han et al.'s work, [48–51,71] we also introduce the nearest-neighbor approximation, which means that only the interaction with the adjacent neighboring molecules is considered. The electronic couplings for hole and electron transfer in the four cases (P, X1, X2, and L) are calculated based on DFT with PW91 functional and TZ2P basis set. It is found that the calculated electronic couplings of the L dimers are very small and negligible, which means that the charge transport in the organic materials is a 2D transport within the stacked organic layers [72,73]. The hole-transport electronic couplings V_h and electron-transport electronic couplings V_e of each packing mode of crystal 1 and 2 are shown in Table 1. One can find that all V_e are larger than V_h (except in the case of the p type packing mode of crystal 2). These results confirm that complex 1 and 2 are favor to be n-type organic semiconductor.

On the other hand, X2 packing mode of crystals 2 produces the largest $V_e = -64.49$ meV, which is about 19 times larger than the counterpart of crystal 1. The different structures of molecules of crystal 1 and 2 are responsible to this significant change. As discussed above, monomers of crystal 1 and 2 are isomer. There's only one little difference of

Table 1
Calculated hole-transport electronic couplings V_h (meV) and electron-transport electronic couplings V_e (meV) for the different hopping pathways in crystal 1 and 2.

Pathway	1		2	
	V_h	V_e	V_h	V_e
P	6.99	−7.94	7.07	−2.72
X1	−2.16	3.15	10.08	−20.16
X2	−13.50	17.24	3.53	−64.49

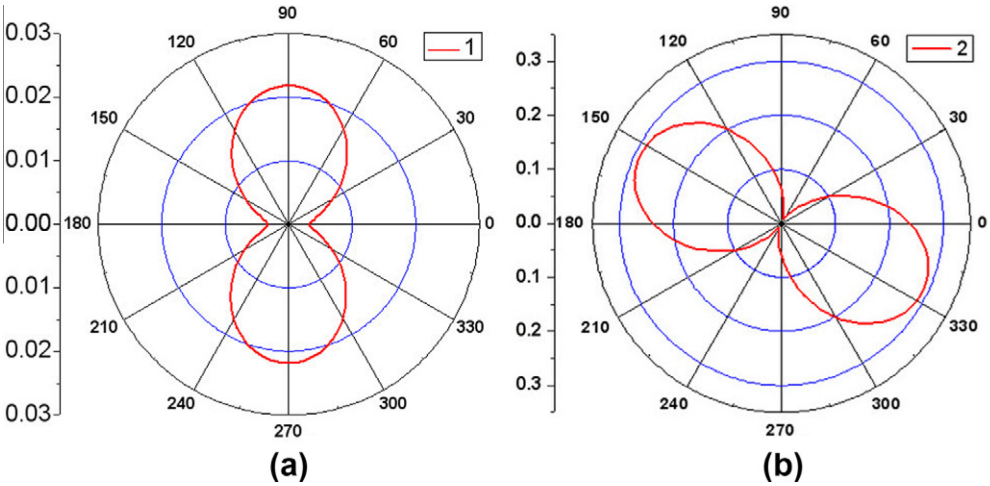

Fig. 5. Calculated angle resolved anisotropic electron mobility of complex 1 and 2, respectively.

their structures that the heterocycle associates with different carbon atoms. However, just this little difference introduces large change of the frontier molecular orbitals. Fig. 3 indicates the frontier molecular orbitals of monomer 1 and 2. It obviously that HOMO of monomer 1 locates at the left part, while that of monomer 2 distributes on the whole molecule. Thus, the extended π-conjugated system is beneficial to electronic coupling between neighbor molecules. Above all, it's indicated that crystal 2 should be function as n-type organic semiconductor material better than crystal 1.

The properties of these two crystals as n-type organic semiconductor material are investigated in detail. In the reference plane a-b of crystal 1, crystal axis a is chose to be the reference axis and Φ is the orientation angle of the transistor channel relative to the reference axis and θ_i are the angles of the projected electronic coupling pathways of different dimer types relative to the reference axis. In crystal 1, the roll angles θ_p of dimers P dimer is 0° and the separating distance is about 9 Å. As shown in Fig. 4(1), the effective coupling projected areas is small, therefore, the electron-transfer mobility at this direction is only about 0.003 $cm^2 V^{-1} s^{-1}$. In the crystal 1, the geometries of X1 and X2 dimers with the roll angles of 29.0 and 90.0°, the separating distances are 10 and 5 Å. With the longest separating distance, X1 dimer provides the smallest the electron-transfer mobility, only about 0.0001 $cm^2 V^{-1} s^{-1}$ because of the small effective coupling projected areas. On the contrary, X2 dimer has the shortest separating distance 5 Å and the electron-transfer mobility is the largest, about 0.022 $cm^2 V^{-1} s^{-1}$. It's more than 7 times of P dimer and 220 times of X1 dimer. In the case of crystal 2, as shown in Fig. 2(2) and Fig. 4(2), plane a-b is the reference plane; crystal axis a is chose to be the reference axis and Φ is the orientation angle of the transistor channel relative to the reference axis and θ_i are the angles of the projected electronic coupling pathways of different dimer types relative to the reference axis. The separating distance of P dimer is about 12 Å which is longer than that of the counterpart of crystal 1. The electron-transfer mobility of P direction is only 4.5682×10^{-6} $cm^2 V^{-1} s^{-1}$, which is far less than that of crystal 1. The separating distance of X1 dimer is about 9 Å which is shorter than that of crystal 1. The electron-transfer mobility of X1 direction is about 0.009 $cm^2 V^{-1} s^{-1}$, which is far bigger than that of crystal 1 (90 times). The largest electron-transfer mobility appears at the X2 direction of crystal 2. It's 0.291 $cm^2 V^{-1} s^{-1}$, about 10 times bigger than that of crystal 1. There are two parameters contribute to this significantly big mobility. One is the short separating distance, about only 5 Å. The other one is the better planar structure of the monomer comparing with crystal 1, which produces larger electronic coupling.

The anisotropic electron-transfer mobility in 1 and 2 single crystals is shown in Fig. 5. Electron-transfer mobility of 2 is obviously larger than that of 1. It can be seen from Fig. 5 that the angle dependence of mobility in 1 and 2 single crystal both shows remarkable anisotropic behavior. But the highest mobility value appears when the value of Φ near 90/270° in crystal 1, while it's 150/330° in crystal 2. The mobility in crystal 2 is larger than crystal 1 with different order of magnitude. This is derived from differences between monomers of these two crystals. Monomers of crystal 1 and 2 have the same formula $C_{26}H_{19}BF_2N_2O_3$, with only one alternation in the structures that the heterocycle associates with different carbon atoms. Just this little change introduces a more planar structure of monomer 2 and the large π-conjugation, which determines the larger mobility of crystal 2, directly.

4. Conclusion

We theoretically investigated two BODIPY derivatives as organic semiconductor. The result indicates that the electron-transport electronic couplings V_e of both complex 1 and 2 are larger than their electron-transport electronic couplings V_h, which means they are favor to be n-type semiconductor. On the other hand, the angle dependence of mobility in 1 and 2 single crystal both shows remarkable anisotropic behavior. However, the maximum mobility of crystal 2 are more than ten times larger than crystal 1. As molecular 1 and 2 are isomeric with only little difference of the structure, this obvious difference of mobility demonstrates that isomerism has significant influence on the properties of organic semiconductor. The result is essential for designing better functional organic semiconductors. As usual, when purify a new material after synthesizing, it's difficult to separate the isomers and get the pure crystal. On the contrary, the isomer of the main product might have some kind of new good function which is different with the main product.

Acknowledgement

This work was supported by NSFC (Nos. 20903094 and 20833008) and NKBRSF (Nos. 2007CB815202 and 2009CB220010).

References

[1] H. Sirringhaus, T. Kawase, R.H. Friend, T. Shimoda, M. Inbasekaran, W. Wu, E.P. Woo, Science 290 (2000) 2123–2126.

[2] H.E. Katz, A.J. Lovinger, J. Johnson, C. Kloc, T. Slegrist, W. Li, Y.Y. Lin, A. Dodabalapur, Nature 404 (2000) 478–481.

[3] G. Yu, J. Gao, J.C. Hummelen, F. Wudl, A.J. Heeger, Science 270 (1995) 1789–1791.

[4] J.H. Burroughes, D.D.C. Bradley, A.R. Brown, R.N. Marks, K. Mackay, R.H. Friend, P.L. Burns, A.B. Holmes, Nature 347 (1990) 539–541.

[5] C.W. Tang, S.A. Vanslyke, Appl. Phys. Lett. 51 (1987) 913–915.

[6] (a) J.L. Brédas, D. Beljonne, V. Coropceanu, J. Cornil, Chem. Rev. 104 (2004) 4971–5003;
(b) J.L. Brédas, J.P. Calbert, D.A. da Silva, J. Cornil, Proc. Natl. Acad. Sci. U.S.A. 99 (2002) 5804–5809.

[7] S. Chai, S.H. Wen, K.-L. Han, Org. Electron. 12 (2011) 1806–1814.

[8] S.F. Nelson, Y.-Y. Lin, D.J. Gundlach, T.N. Jackson, Appl. Phys. Lett. 72 (1998) 1854–1856.

[9] V.C. Sundar, J. Zaumseil, V. Podzorov, E. Menard, R.L. Willett, T. Someya, M.E. Gershenson, J.A. Rogers, Science 303 (2004) 1644–1646.

[10] V. Podzorov, E. Menard, J.A. Rogers, M.E. Gershenson, Phys. Rev. Lett. 95 (2005) 226601.

[11] V. Podzorov, E. Menard, A. Borissov, V. Kiryukhin, J.A. Rogers, M.E. Gershenson, Phys. Rev. Lett. 93 (2004) 086602.

[12] L. Li, M. Debucquoy, J. Genoe, P. Heremans, J. Appl. Phys. 107 (2010) 24519.

[13] M. Linares, D. Beljonne, J. Cornil, K. Lancaster, J.L. Brédas, S. Verlaak, A. Mityashin, P. Heremans, A. Fuchs, C. Lennartz, J. Ide, R. Mereau, P. Aurel, L. Ducasse, F. Castet, J. Phys. Chem. B. 114 (2010) 3215–3224.

[14] C. Rolin, K. Vasseur, J. Genoe, P. Heremans, Org. Lett. 11 (2010) 100–108.

[15] S. Verlaak, D. Beljonne, D. Cheyns, C. Rolin, M. Linares, F. Castet, J. Cornil, P. Heremans, Adv. Funct. Mater. 19 (2009) 3809–3814.

[16] Cheyns, D., Gommans, H., Odijk, M., Poortmans, J., Heremans, P. Sol. Energy Mater. Sol. Cells 91 (2007) 399–404.

[17] S. Steudel, D. Janssen, S. Verlaak, J. Genoe, P. Heremans, Appl. Phys. Lett. 85 (2004) 5550–5552.

[18] R. Ruiz, B.A. Nickel, N. Koch, G. Scoles, L.C. Feldman, R.F. Haglund, A. Kahn, Phys. Rev. B 67 (2003) 125406.

[19] I.G. Hill, J. Hwang, C. Huang, A. Kahn, J.E. McDermott, J. Schwartz, Appl. Phys. Lett. 90 (2007) 012109.

[20] N.E. Gruhn, D.A. Filho, T.G. Bill, M. Malagoli, A. Kahn, J.L. Brédas, J. Am. Chem. Soc. 124 (2002) 7918–7919.

[21] F. Amy, C. Chan, A. Kahn, Org. Electron. 6 (2005) 85–91.

[22] C.K. Chan, A. Kahn, Appl. Phys. A 95 (2009) 7–13.

[23] W. Zhao, Y.B. Qi, T. Sajoto, S. Barlow, S.R. Marder, A. Kahn, Appl. Phys. Lett. 97 (2010) 123305.

[24] K. Harada, M. Sumino, C. Adachi, S. Tanaka, K. Miyazaki, Appl. Phys. Lett. 96 (2010) 253304.

[25] H.Y. Chen, I. Chao, Chem. Phys. Lett. 401 (2005) 539–545.

[26] M.Y. Kuo, H.Y. Chen, I. Chao, Chem. Eur. J. 13 (2007) 4750–4758.

[27] Y.C. Chang, I. Chao, J. Phys. Chem. Lett. 1 (2010) 116–121.

[28] W.Q. Deng, W.A. Goddard III, J. Phys. Chem. B 108 (2004) 8614–8621.

[29] V. Coropceanu, J. Cornil, D.A. da Silva Filho, Y. Olivier, R. Silbey, J.L. Brédas, Chem. Rev. 107 (2007) 926–952.

[30] G.R. Hutchison, M.A. Ratner, T.J. Marks, J. Am. Chem. Soc. 127 (2005) 2339–2350.

[31] G. Yu, S.W. Yin, Y.Q. Liu, Z.G. Shuai, D.B. Zhu, J. Am. Chem. Soc. 125 (2003) 14816–14824.

[32] H. Chen, M. Shi, T. Aernouts, W. Wang, G. Borghs, P. Heremans, Sol. Energy Mater. Sol. Cells 87 (2005) 521–527.

[33] S. Schols, L. Van Willigenburg, R. Mueller, D. Bode, M. Debucquoy, S. De Jonge, J. Genoe, P. Heremans, S. Luyten, A. Facchetti, Appl. Phys. Lett. 93 (2008) 263303.

[34] C.K. Chan, F. Amy, Q. Zhang, S. Barlow, S. Marder, A. Kahn, Chem. Phys. Lett. 431 (2006) 67–73.

[35] C. Chan, E.G. Kim, J.L. Brédas, A. Kahn, Adv. Funct. Mater. 16 (2006) 831–837.

[36] D. Matsuo, X. Yang, A. Hamada, K. Morimoto, T. Kato, M. Yahiro, C. Adachi, A. Orita, J. Otera, Chem. Lett. 39 (2010) 1300–1302.

[37] J.Y. Lee, S. Roth, Y.W. Park, Appl. Phys. Lett. 88 (2006) 252106.

[38] M.M. Ling, C. Reese, A.L. Briseno, Z. Bao, Synth. Met. 157 (2007) 257–262.

[39] S.C.B. Mannsfeld, J. Locklin, C. Reese, M.E. Roberts, A.J. Lovinger, Z. Bao, Adv. Funct. Mater. 17 (2007) 1617–1622.

[40] C. Reese, Z. Bao, Adv. Mater. 19 (2007) 4535–4538.

[41] O. Ostroverkhova, D.G. Cooke, F.A. Hegmann, R.R. Tykwinski, S.R. Parkin, J.E. Anthony, Appl. Phys. Lett. 89 (2006) 192113.

[42] R.L. Headrick, S. Wo, F. Sansoz, J.E. Anthony, Appl. Phys. Lett. 92 (2008) 063302.

[43] K. Hannewald, P.A. Bobbert, Phys. Rev. B 69 (2004) 075212.

[44] S.W. Yin, Y.F. Lv, Org. Electron. 9 (2008) 852–855.

[45] G.A. de Wijs, C.C. Mattheus, R.A. de Groot, T.T.M. Palstra, Synth. Met. 139 (2003) 109–114.

[46] Y.K. Lan, C.I. Huang, J. Phys. Chem. B 112 (2008) 14857–14862.

[47] Y.X. Zhang, X. Cai, D.D. Qi, Y.Z. Bian, J.Z. Jiang, J. Phys. Chem. C 112 (2008) 14579–14588.

[48] S.H. Wen, W.Q. Deng, K.L. Han, Chem. Commun. 46 (2010) 5133–5135.

[49] S.H. Wen, A. Li, J.L. Song, W.Q. Deng, K.L. Han, W.A. Goddard III, J. Phys. Chem. B 113 (2009) 8813–8819.

[50] J.D. Huang, S.H. Wen, W.Q. Deng, K.L. Han, J. Phys. Chem. B 115 (2011) 2140–2147.

[51] S.H. Wen, W.Q. Deng, K.L. Han, Phys. Chem. Chem. Phys. 12 (2010) 9267–9275.

[52] A. Loudet, K. Burgess, Chem. Rev. 107 (2007) 4891–4932.

[53] A. Coskun, E.U. Akkaya, J. Am. Chem. Soc. 127 (2005) 10464–10465.

[54] Y. Gabe, Y. Urano, K. Kikuchi, H. Kojima, T. Nagano, J. Am. Chem. Soc. 126 (2004) 3357–3367.

[55] A. Hepp, G. Ulrich, R. Schmechel, H. von Seggern, R. Ziessel, Synth. Met. 146 (2004) 11–15.

[56] R. Ziessel, G. Ulrich, A. Harriman, New J. Chem. 31 (2007) 496–501.

[57] N. Saki, T. Dinc, E.U. Akkaya, Tetrahedron 62 (2006) 2721–2725.

[58] Y. Zhou, Y. Xiao, S.M. Chi, X.H. Qian, Org. Lett. 10 (2008) 633–636.

[59] R.A. Marcus, J. Chem. Phys. 24 (1956) 966–978.

[60] N.S. Hush, J. Chem. Phys. 28 (1958) 962–972.

[61] E.F. Valeev, V. Coropceanu, D.A. da Silva, S. Salman, J.L. Bredas, J. Am. Chem. Soc. 128 (2006) 9882–9886.

[62] G.T. Velde, F.M. Bickelhaupt, E.J. Baerends, C.F. Guerra, S.J.A. Van Gisbergen, J.G. Snijders, T.J. Ziegler, J. Comput. Chem. 22 (2001) 931–967.

[63] V. Lemaur, D.A. Da Silva Filho, V. Coropceanu, M. Lehmann, et al., J. Cornil, J. Am. Chem. Soc. 126 (2004) 3271–3279.

[64] M.J. Frisch, G.W. Trucks, H.B. Schlegel, G.E. Scuseria, M.A. Robb, J.R. Cheeseman, J.A. Montgomery, T. Vreven, K.N. Kudin, J.C. Burant, J.M. Millam, S.S. Iyengar, J. Tomasi, V. Barone, B. Mennucci, M. Cossi, G. Scalmani, N. Rega, G.A. Petersson, H. Nakatsuji, M. Hada, M. Ehara, K. Toyota, R. Fukuda, J. Hasegawa, M. Ishida, T. Nakajima, Y. Honda, O. Kitao, H. Nakai, M. Klene, X. Li, J. E. Knox, H.P. Hratchian, J.B. Cross, C. Adamo, J. Jaramillo, R. Gomperts, R.E. Stratmann, O. Yazyev, A.J. Austin, R. Cammi, C. Pomelli, J.W. Ochterski, P.Y. Ayala, K. Morokuma, G.A. Voth, P. Salvador, J.J. Dannenberg, V.G. Zakrzewski, S. Dapprich, A.D. Daniels, M.C. Strain, O. Farkas, D.K. Malick, A.D. Rabuck, K. Raghavachari, J.B. Foresman, J.V. Ortiz, Q. Cui, A.G. Baboul, S. Clifford, J. Cioslowski, B.B. Stefanov, G. Liu, A. Liashenko, P. Piskorz, I. Komaromi, R.L. Martin, D.J. Fox, T. Keith, M.A. Al-Laham, C.Y. Peng, A. Nanayakkara, M. Challacombe, P.M.W. Gill, B. Johnson, W. Chen, M.W. Wong, C. Gonzalez, J.A. Pople, Gaussian03; Gaussian, Inc.: Wallingford, CT, 2004.

[65] E.A. Silinsh, V. Capek, Organic Molecular Crystals: Interaction, Localization, and Transport Phenomena, New York, 1994.

[66] N. Sato, K. Seki, H. Inokuchi, J. Chem. Soc. 77 (1981) 1621–1633.

[67] E.G. Kim, V. Coropceanu, N.E. Gruhn, R.S. Sanchez-Carrera, R. Snoeberger, A.J. Matzger, J.L. Bredas, J. Am. Chem. Soc. 129 (2007) 13072–13081.
[68] R.A. Marcus, Rev. Mod. Phys. 65 (1993) 599–610.
[69] S. Mohakud, A.P. Alex, S.K. Pati, J. Phys. Chem. C 114 (2010) 20436–20442.
[70] A. Chandekar, J.E. Whitten, Synth. Met. 150 (2005) 259–264.
[71] S. Chai, S.H. Wen, J.D. Huang, K.L. Han, J. Comput. Chem. 32 (2011) 3218–3225.
[72] V. Coropceanu, J. Cornil, D.A da Silva, Y. Olivier, R. Silbey, J.L. Bredas, Chem. Rev. 107 (2007) 2165.
[73] X.D. Yang, L.J. Wang, C.L. Wang, W. Long, Z.G. Shuai, Chem. Mater. 20 (2008) 3205–3211.